Results in Physics 16 (2020) 103002

Contents lists available at ScienceDirect

Results in Physics

journal homepage: www.elsevier.com/locate/rinp

Luminescence and vacuum ultraviolet excitation spectroscopy of cerium doped $Gd_3Ga_3Al_2O_{12}$ single crystalline scintillators under synchrotron radiation excitations

Anna P. Kozlova[a], Valentina M. Kasimova[a], Oleg A. Buzanov[b], Kirill Chernenko[c], Konstantin Klementiev[c], Vladimir Pankratov[d,*]

[a] National University of Science and Technology "MISiS", Leninsky Prospekt 4, 119049 Moscow, Russia
[b] OJSC "Fomos-Materials" Co., Buzheninova Street 16, 107023 Moscow, Russia
[c] MAX IV Laboratory, Lund University, PO BOX 118, SE-221 00 Lund, Sweden
[d] Institute of Solid State Physics, University of Latvia, 8 Kengaraga iela, LV-1063 Riga, Latvia

ARTICLE INFO

Keywords:
$Gd_3Ga_3Al_2O_{12}$
Ce^{3+}
VUV spectroscopy
Luminescence
XANES
Synchrotron radiation

ABSTRACT

Cerium doped $Gd_3Ga_3Al_2O_{12}$ (GGAG) single crystals as well as GGAG:Ce single crystals co-doped by divalent (Mg^{2+}, Ca^{2+}), trivalent (Sc^{3+}) or tetravalent (Zr^{4+}, Ti^{4+}) ions have been studied by means of the excitation luminescence spectroscopy in vacuum ultraviolet spectral range. Synchrotron radiation from the undulator beam was utilized for the luminescence excitation in the energy range from 4.5 to 800 eV. The influence of the co-dopant ions on the excitonic transitions as well as on the intrinsic defects in GGAG was revealed examining the luminescence emission and excitation spectra of both Gd^{3+} and Ce^{3+} ions in all single crystals studied. Special attention was paid to the analysis of Ce^{3+} excitation spectra in VUV spectral range (4.5–45 eV) where multiplication of electronic excitation (MEE) processes occur. It was obtained that GGAG:Ce single crystals having different co-dopant ions reveal distinguished efficiency of MEE. The role of intrinsic defects in MEE processes in the co-doped GGAG:Ce single crystals was elucidated.

Introduction

Cerium doped Gallium Gadolinium Aluminum Garnet ($Gd_3Ga_3Al_2O_{12}$:Ce or GGAG:Ce) nowadays is one of the most popular scintillation material. GGAG:Ce demonstrates excellent light output of scintillations (58,000 photons/MeV) [1] and, therefore, it is considered to be as one of the most prospective scintillators in high energy physics [1–3] as well as in medical applications [1,4]. The GGAG:Ce compound was patented in 2006 by Kanai et al. [5], however, the first GGAG:Ce single crystal was grown only in 2011 by the Czochralski method [6]. Later on GGAG:Ce single crystals were also successfully grown by the same authors using micropulling down method [7]. Despite of many excellent scintillating properties of the GGAG:Ce such as a high light output, high density (6.63 g/cm^3) and fast decay time (90 ns) [8–10] the practical application is limited due to a relatively long afterglow of Ce^{3+} emission in this single crystal. The existence of slow decay components of Ce^{3+} emission in GGAG can be explained by the intermediate localization of the charge carriers at shallow traps during energy transfers to the Ce^{3+} emission centers. In order to suppress the slow components of Ce^{3+} emission decay it was suggested to co-dope the GAGG:Ce single crystals by divalent ions [9,11,12]. The most pronounced effect was achieved for the crystals co-doped with Mg^{2+} or Ca^{2+} ions [13]. It was supposed that the co-doping by divalent ions allows to change the valence of cerium ions from 3+ to 4+ and accelerates the energy transfer processes to emission centers in garnets [11,14,15]. However, the co-doping of the GGAG:Ce crystals by divalent ions significantly suppresses the scintillation light yield presumably due to the shift of 5d levels of Ce^{3+} towards the bottom of the conduction band as well as because of the appearance of the deep traps induced by the co-dopant ions. Therefore, in order to identify the influence of co-dopant ions on the luminescence properties of GGAG:Ce single crystals it is necessary to tune excitation energy from the energy which corresponds to the direct excitation of Ce^{3+} ion to excitonic and band-to-band transitions energies. GGAG compound belongs to the class of wide band gap materials having the forbidden gap about 6 eV. This energy and higher refers to the vacuum ultraviolet (VUV) spectral range. The most suitable excitation source in VUV range is synchrotron radiation, which was successfully utilized for the VUV excitation

* Corresponding author.
E-mail address: vladimirs.pankratovs@cfi.lu.lv (V. Pankratov).

https://doi.org/10.1016/j.rinp.2020.103002
Received 22 November 2019; Received in revised form 7 February 2020; Accepted 8 February 2020
Available online 12 February 2020

spectroscopy of wide band gap materials [16–19] and semiconductors [20–22].

A tuneability of synchrotron radiation allows to excite samples by high-energy photons, which corresponds to the energy of hot charge carriers as well as to the energy when multiplication of electronic excitation processes take place. The thermalization processes of electrons and holes as well as the multiplications of electronic excitations are extremely important for the elucidating of energy transfer processes in scintillators. The influence of co-dopant ions in GGAG:Ce on the thermalization and multiplication processes has not been studied so far. In the current paper we report pioneering results of VUV luminescence spectroscopy under synchrotron radiation excitations of co-doped GGAG:Ce single crystals. The origin of the modification of energy transfer efficiency to the emission center in the co-doped GGAG:Ce single crystals is discussed in the paper. Furthermore, the changes of the energy bands structure in the excitonic region as well as the excitation bands due to defects induced by co-dopant ions are demonstrated.

Experimental

Cerium doped GGAG as well as co-doped by several different elements (Mg^{2+}, Ca^{2+}, Sc^{3+}, Zr^{4+}, $Mg^{2+}+Ti^{4+}$) single crystals were grown by Czochralski method in OJSC "Fomos-Materials" (Moscow, Russia). The details of crystals' growth of doped and co-doped GGAG single crystals have been reported in Ref. [23]. The cerium concentration was 3 at.% in all crystals studied. The concentrations of the co-dopants in the GGAG:Ce single crystals were following: 350 ppm (Mg^{2+}), 150 ppm (Ca^{2+}), 100 ppm (Zr^{4+}) and 80 ppm + 30 ppm (Mg^{2+} + Ti^{4+}). The scandium containing crystal was grown according to the chemical composition $Gd_{(3-x)}Ce_xAl_{1,5}Sc_1Ga_{2,5}O_{12}$. The crystals have been cut in small thin plates and polished for optical experiments. Nominally pure GGAG single crystal was also measured for comparison.

The main characterization method utilized in current study is a luminescence spectroscopy under synchrotron radiation excitation. These experiments have been carried out on the photoluminescence endstation [24] of the FinEstBeAMS undulator beamline [25], which was recently constructed and developed at 1.5 GeV storage ring of MAX IV synchrotron facility (Lund, Sweden). The excitation energy range was 4.5–800 eV, while temperature was varied from 10 to 300 K. The excitation spectra were normalized utilizing the calibration curve obtained by means of AXUV-100G diode. In order to suppress high orders of excitation at the FinEstBeAMS beamline a set of the filters (fused silica, MgF_2, In, Sn, Mg and Al) has been chosen, which is covering the excitation spectral range in question. Luminescence detection in UV–visible spectral range (200–800 nm) was performed by an Andor Shamrock (SR-303i) 0.3 m spectrometer equipped with two gratings (300 l/mm) optimized for different spectral regions (300 and 500 nm blaze, respectively). The Andor Shamrock spectrometer was equipped with two easily replaceable photomultipliers (H8259 and H8259-01 Hamamatsu photon counting heads) covering the spectral range from 185 to 900 nm. The emission spectra were corrected for the spectral sensitivity of the detection system.

In order to identify Ce^{3+} and Ce^{4+} content in the crystals, X-ray absorption experiments were carried out on the BALDER beamline at 3.0 GeV storage ring of MAX IV Laboratory [26]. The XANES spectra were measured in fluorescence detection mode by a 7-element silicon drift detector. Continuous energy scanning was performed at a speed ~5 s/XANES. For each sample, 25 repeats were examined for possible radiation damage and afterwards accumulated into a resulting spectrum. The reference CeO_2 sample was measured in transmission mode in order to avoid self-absorption distortion in such a concentrated sample (this effect is absent in the low-concentrated GGAG crystals).

Results and discussion

The Fig. 1 depicts the comparison of the emission spectra for the set of co-doped GGAG:Ce single crystals at low temperature under deep VUV (45 eV) excitation. Each emission spectrum reveals a sharp line at 317 nm and a broad band in the green-yellow spectral range. The 317 nm emission results from $^6P_{7/2} \rightarrow {}^8S_J$ radiative transition of Gd^{3+} ion, whereas the broad band is due to 5d-4f transition in Ce^{3+}. We have not compared a light output of the crystals; therefore, the spectra are normalized at the maximum intensity of the Ce^{3+} emission bands. It is clearly seen (Fig. 1) that Ce^{3+} emission bands are influenced by some of the co-dopants. Ca^{2+} and Sc^{3+} impurities induce the most noticeable changes shifting the Ce^{3+} emission spectra towards the low energy side compared to the corresponding spectrum in GGAG:Ce crystal (black line). On the other hand, the Ce^{3+} emission spectrum of the Mg^{2+} co-doped crystal is practically the same as in the non-co-doped crystal. The reason of the observed changes in the emission spectra can be connected with the perturbation of the crystal field by co-dopant ions affecting *5d* levels of Ce^{3+}. The ionic radii of Ca^{2+} is 1.04 Å and it is the biggest among the co-dopant ions (Sc^{3+}, Zr^{4+} have 0.83 and 0.82 Å, respectively) [27], whereas the Mg^{2+} has the smallest one (0.74 Å) and does not noticeably perturb the energy levels of Ce^{3+} [28]. It means that there is a correlation of the ionic radii of the co-dopant ions and the perturbation of the crystal field leading to the shifts of the Ce^{3+} emission bands. In fact, the introducing of the co-dopant into the melt can slightly change Al/Ga ratio in the final crystal. Indeed, manipulating the Al/Ga ratio in GGAG:Ce one can tune the band gap of this compound as well as change the Ce^{3+} levels in the forbidden gap [29]. The red shift of the Ce^{3+} emission spectra occurs if the ratio of the Al/Ga increases [30]. Therefore, the observed red shift in the emission spectra (Fig. 1) can be explained by the slight influence of the Ca^{2+}, Sc^{3+} and Zr^{4+} co-dopants on the stoichiometry in the corresponding crystals.

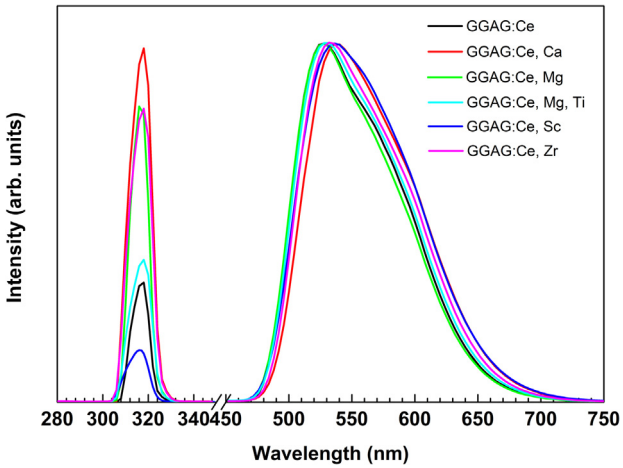

Fig. 1. The luminescence spectra of the GGAG:Ce as well as of the GGAG:Ce co-doped single crystals under 45 eV excitation at 10 K. The spectra are normalized at maximum intensity of Ce^{3+} emission band.

Low temperature experiments allow us to detect also Gd^{3+} lines, which are completely quenched at room temperature [31]. It is clearly seen that the intensity ratio of the Ce^{3+}/Gd^{3+} emissions is different for the crystals having different co-dopants content. If one considers Gd^{3+} and Ce^{3+} emissions as two competing radiative relaxation channels, Fig. 1 preliminary demonstrates the influence of the co-dopants on the energy transfer processes from host lattice to Ce^{3+} in GGAG crystals. For instance, taking into account that the cerium concentration was the same in all crystals studied, one would tentatively suggest that the Ca^{2+} co-doped crystal has the lowest efficiency of energy transfer to Ce^{3+} center among all co-doped crystals because it has the smallest Ce^{3+}/Gd^{3+} ratio of the corresponding emission intensities.

To highlight the energy transfer processes in details the excitation spectra of both Ce^{3+} and Gd^{3+} have been measured in wide spectral range for all crystals studied. The GGAG:Ce crystals studied do not show

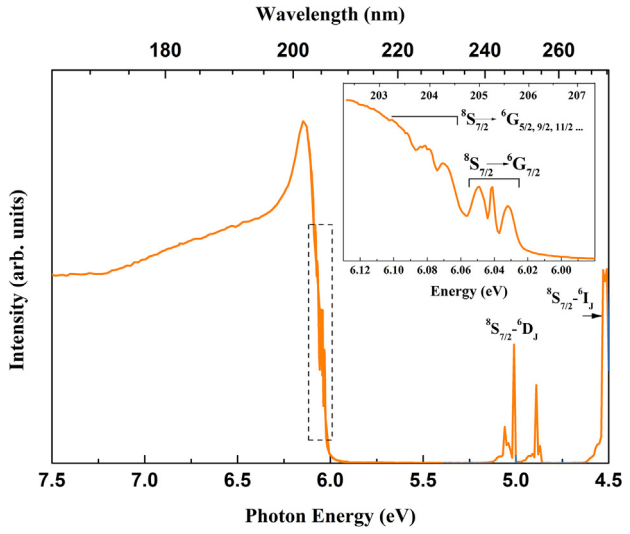

Fig. 2. The excitation spectrum of the Gd^{3+} in the undoped GGAG single crystal monitoring the emission at 317 nm ($^6P_{7/2} \rightarrow {}^8S_{7/2}$) at 10 K. The dashed area is shown in details inset.

any intrinsic emissions related to self-trapped or bound excitons even at low temperature. Furthermore, the luminescence of intrinsic (*antisite*) defects is typical for garnet crystals like YAG [32,33] or LuAG [34]. However, we have not detected any intrinsic luminescence even in the nominally pure GGAG crystals. Therefore, Gd^{3+} emission is the only competitive radiative relaxation channel in the crystals studied. The excitation spectrum of the Gd^{3+} (317 nm) of the nominally pure GGAG single crystal is shown in Fig. 2. The spectrum reveals a well-resolved excitonic peak at 6.15 eV with subsequent intensity drop down to 70–75% comparing to the intensity of the excitonic peak. The fine structure can be resolved on the excitonic peak's background (Fig. 2 inset). This fine structure is due to $^8S_{7/2} \rightarrow {}^6G_J$ transitions in Gd^{3+} ions and it can be observed later on in all GGAG crystals excepting the Sc^{3+} doped sample.

The comparison of the excitation spectra of Gd^{3+} luminescence (317 nm) in the low energy (excitonic) range is demonstrated in Fig. 3 for all GGAG:Ce single crystals studied. All spectra are normalized at the maximum intensity. Considering these excitation spectra (Fig. 3) one can see that excitonic peak position is sample dependent. The main excitonic peaks for both GGAG:Ce and Ca^{2+} co-doped crystals are

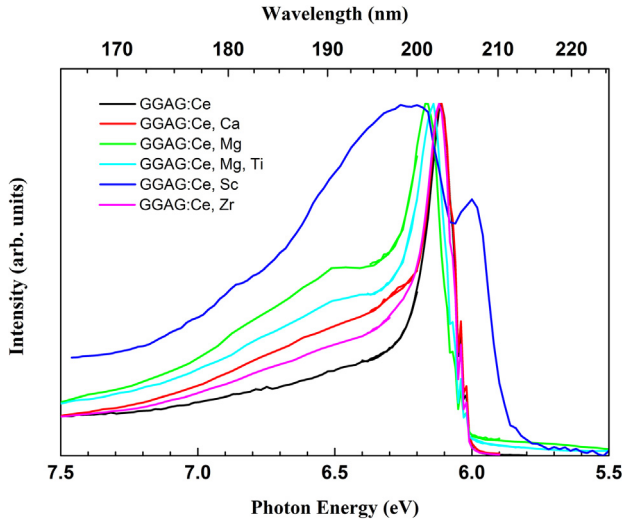

Fig. 3. The excitation spectra of the Gd^{3+} in the GGAG:Ce single crystals monitoring the emission at 317 nm ($^6P_{7/2} \rightarrow {}^8S_{7/2}$) at 10 K.

almost the same peaking at 6.1 eV. The excitonic peak of the Zr^{4+} co-doped crystal is insignificantly shifted towards to the high-energy side, peaking at 6.12 eV. The blue shifts of the excitonic peaks are more pronounced in the excitation spectra of Mg^{2+} and Mg + Ti co-doped crystals. These excitonic peaks are observed at 6.16 eV and 6.14 eV, respectively. However, the most evident changes are observed in the excitation spectrum of the Sc^{3+} co-doped crystal. Indeed, the excitonic peak is strongly redshifted (6.0 eV) for this crystal. Furthermore, there is a distinguished shape of the excitation spectrum for the Sc^{3+} co-doped crystal at energies higher than the excitonic peak's position, i.e. there is an intensive excitation upsurge starting from 6.1 eV with subsequent intensity degradation at energy higher than 6.3 eV. All other excitation spectra in Fig. 3 (except the spectrum for the Sc^{3+} co-doped crystal) demonstrate intensity decline at energies exceeding the excitonic peak position. From this point of view, these spectra are similar to the excitation spectrum of the nominally pure GGAG (Fig. 2). However, the intensity's drop in the cerium doped crystals is much stronger than it was observed in the nominally pure crystal (Fig. 2). For example, the intensity of the signal at 6.3 eV in the GAGG:Ce is only about 25–30% from the intensity of the corresponding excitonic peak, whereas this value was 70–75% in the nominally pure GGAG crystal (Fig. 2). The strong intensity decrease in the excitation spectra of the Gd^{3+} emission in the cerium doped crystals at energies exceeding excitonic energy can be explained by an efficient energy transfer from host lattice to Ce^{3+} ions. On the other hand, the energy transfer is affected by co-doping impurities because the shapes of the excitation spectra of Gd^{3+} emission are different for co-doped crystals in the 6.3–7.5 eV spectral range.

The excitation spectra of Ce^{3+} emission are shown in Fig. 4 for all crystals studied. These spectra in the excitonic range are similar to the corresponding excitation spectra of Gd^{3+} emission (Fig. 3). Indeed, the spectrum of Mg^{2+} co-doped crystal is most blue shifted among others Ce^{3+} excitation spectra, while Sc^{3+} doped crystal reveals a relatively strong red shift of the excitonic band. The co-doping by other co-dopants also leads to small deviation of the excitonic band from the position of that one in the non-co-doped crystals. Analyzing the excitation spectra of both emissions (Gd^{3+} and Ce^{3+}) in the spectral range close to the excitonic transitions we can suggest that co-doped ions slightly modify the stoichiometry of the crystals. In fact, by introducing a co-dopant ion into the GGAG lattice and substituting ions in the lattice one can slightly change Ga/Al ration as well as the content of Gd^{3+} in the

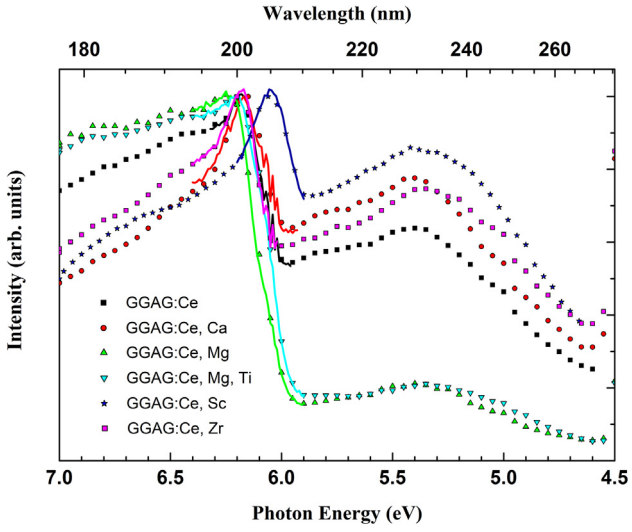

Fig. 4. The excitation spectra of Ce^{3+} emission (530 nm) in the GGAG:Ce crystals at 10 K. The lines of the corresponding colors are needed for better visualization of the excitonic bands as well as the fine structures due to Gd^{3+} transitions.

lattice. Both of these factors influence an electronic structure of the GGAG changing band gap based on the concept of the band gap engineering in garnets [29,30,35]. The most evident excitonic peak's shift is observed in the spectrum of Sc^{3+} doped crystal. There is the highest co-dopant concentration leading to the strongest band gap modification in this crystal among all samples studied.

Next, we are focusing on the low energy part of the excitation spectra in Fig. 4. Each excitation spectrum contains the wide excitation band at energies below excitonic transitions (4.5–6.0 eV range). On the other hand, based on the literature data [13], the absorption band caused by Ce^{4+} center in GGAG is located in this spectral range too. This absorption band results due to electron transfer from the valence band to the ground state of Ce^{4+} forming Ce^{3+} in ground state. It means that a direct excitation in Ce^{4+} absorption band does not lead to Ce^{3+} emission. Thus, Ce^{4+} ion and a center responsible for the excitation band in 4.5–6.0 eV range (Fig. 4) compete to each other and the crystals with a higher Ce^{4+} concentration should have a lower intensity of the excitation band in 4.5–6.0 eV range. It would be reasonable to expect that the crystal co-doped by divalent ions should have the highest Ce^{4+} concentration because such center can easy compensate a lack of positive charge when a divalent ion substitutes a trivalent one. However, Fig. 4 demonstrates that the intensity of the low-energy excitation band randomly depends on the crystals co-doping. For instance, the intensity of the excitation band peaking at about 5.3 eV is higher in the excitation spectrum of the Sc^{3+} co-doped crystal if to compare with the corresponding band in the non-co-doped crystal. Taking into account that Sc^{3+} substitutes a trivalent ion in GGAG lattice the suppression of Ce^{4+} in scandium doped GGAG crystal looks strange. Furthermore, the substitution of trivalent ion by Zr^{4+} induces one extra positive charge into the crystal lattice. It means that any conditions for the creation of Ce^{4+} centers in Zr^{4+} co-doped crystal should be eliminated and it was expected that the intensity of the 5.3 eV excitation band should be the highest one among all GGAG crystals studied. Instead, we observed that the intensity of the 5.3 eV excitation band for the Zr^{4+} co-doped crystal is quite similar with the intensity of the corresponding band in the Ca^{2+} co-doped sample where Ce^{4+} centers are supposed to be dominant charge compensators. Finally yet importantly, the intensity of the excitation band at 5.3 eV is the smallest for the Mg^{2+} containing samples. The co-doping by Mg^{2+} should efficiently generate Ce^{4+} as Ca^{2+} can do it [14]. However, the intensity of the excitation band at 5.3 eV is three times less in the Mg^{2+} co-doped crystal than in the Ca^{2+} co-doped one. Furthermore, the GGAG:Ce single crystal co-doped by Mg + Ti ions has almost the same excitation spectrum as the Mg^{2+} co-doped single crystal has. It would be reasonably suggested that Ti^{4+} compensates the lack of the positive charge induced by Mg^{2+} ion. In this case the charge state of cerium ions remains unchanged, i.e. as Ce^{3+}. If the co-dopant ions can manipulate the charge state of cerium ion the intensity of this excitation band should be sensitive in respect of the existence of Ti^{4+} ions in the Mg^{2+} co-doped GGAG:Ce single crystals.

In order to identify Ce^{4+} centers in the Mg^{2+} and Ca^{2+} co-doped GGAG crystals the cerium L_{III}-edge XANES spectra have been measured at room temperature and the results are depicted in Fig. 5. The main peak (A) is well-known XANES peak of Ce^{3+} ion [36] is seen in all GGAG:Ce crystals measured, whereas the reference sample (CeO_2) reveals two bands (B and C) which are responsible for Ce^{4+} ion [13,37]. Comparing the XANES data for the GGAG crystals and the CeO_2 reference sample one can conclude that Mg^{2+} co-doped GGAG crystal has some amount of Ce^{4+} ions. Indeed, the XANES spectrum of this crystal clearly contains the band C of Ce^{4+} ion, whereas the intensive peak of Ce^{3+} most likely covers another component (band B) of the Ce^{4+}. The existence of the Ce^{4+} ion in GGAG:Ce co-doped single crystal to our knowledge is a new result. So far it was not strongly established that Mg^{2+} co-doping of GGAG:Ce single crystals leads to the formation of Ce^{4+} ions in GGAG:Ce [38] as well as in other cerium doped scintillators [39]. In contrast to the Mg^{2+} co-doped crystal, the XANES

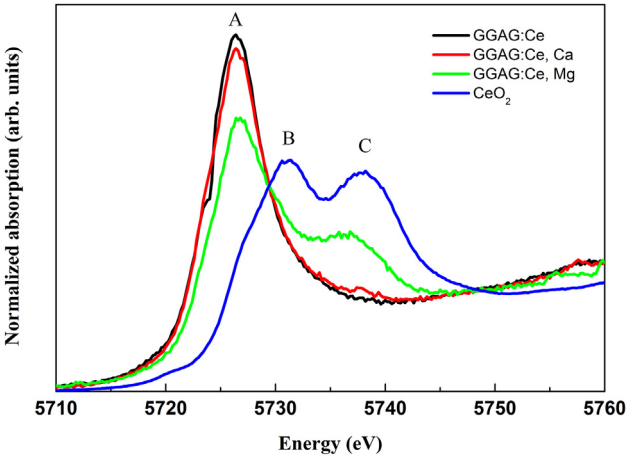

Fig. 5. Cerium L_{III}-edge XANES spectra of GGAG:Ce, GGAG:Ce,Ca^{2+} and GGAG:Ce,Mg^{2+} single crystals. The spectrum of the CeO_2 sample is a reference for Ce^{4+} centers.

spectrum of the Ca^{2+} co-doped crystal practically does not demonstrate any signal due to Ce^{4+} in Fig. 5. Only some traces of the band C can be tentatively resolved. One of the reasons in our opinion could be a low Ca^{2+} concentration in the corresponding crystal. Furthermore, the XANES results obtained (Fig. 5) correlate with the intensity of the 5.3 eV excitation band (Fig. 4) for the Mg^{2+} and Ca^{2+} co-doped crystals supporting the conclusion that the concentration of Ce^{4+} centers is higher in those crystals which reveal smaller intensity of the 5.3 eV excitation band. We suggest that this excitation band is due to some intrinsic defects in GGAG lattice. It can explain a random behavior of the 5.3 eV excitation band in respect of other co-dopant impurities.

Furthermore, we consider the excitation spectra of Ce^{3+} emission in the crystals studied at energies higher than the energy of excitonic transitions in GGAG. Already in the 6.0–70 eV spectral range (Fig. 4) there is an evident difference in the excitation curves among all crystals studied. Fig. 6 demonstrates the same excitation spectra in the extended excitation range up to 45 eV. All excitation spectra show the common behavior. There is excitation intensity degradation at energies just above the energy of band-to-band transitions reaching minimum value at about 10 eV. Note, this intensity decrease is sample dependent. The most precipitous intensity drop is observed in the Sc^{3+} co-doped

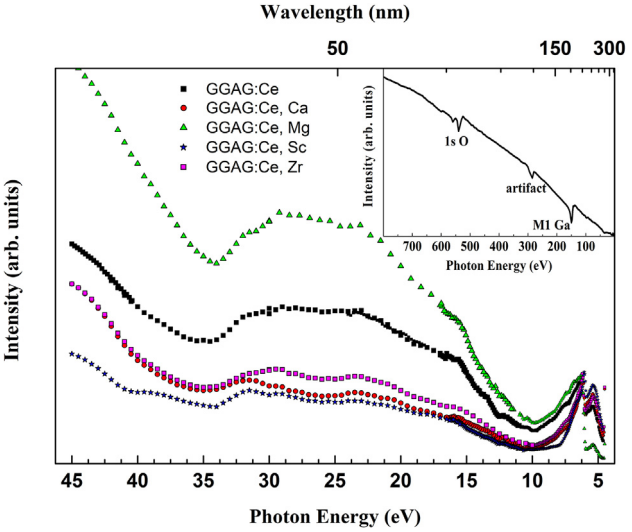

Fig. 6. The excitation spectra of Ce^{3+} emission (530 nm) in the GGAG:Ce crystals at 10 K. The excitation spectrum extended to 800 eV for the GGAG:Ce non-co-doped single crystal is shown inset.

crystal, while the spectrum of the Mg^{2+} co-doped sample is most gently sloped among all crystals. Afterwards, the excitation intensity is rising up at energy at about 12–13 eV in all excitation spectra. This energy range roughly corresponds to the value of $2E_g$ in GGAG, where E_g is a band gap energy. It means that the multiplication of electronic excitations (MEE) processes occur. MEE processes' creation means that two or more luminescence centers are created per one absorbed photon during inelastic electro-electron scattering. For a successful realization of MEE processes, the excitation energy of the photon must exceed a threshold energy, which is $2E_g$ [40–42]. If energy of hot electrons is higher, more secondary electrons can be created and subsequently more luminescence centers can be exited. Fig. 6 (inset) shows the example of the excitation spectrum of Ce^{3+} emission in GGAG:Ce under excitation energy up to 800 eV.

The excitation spectra in Fig. 6 have similar peculiarities in the spectral range 10–45 eV. However, the excitation intensity differs significantly for different crystals. It means that the efficiency of MEE processes is sample dependent. One of the possible explanations is that the co-dopant ion can influence a thermalizataion length in the crystals. The thermalization length is a distance between thermalized geminate electrons and holes and it depends on several factors. One of them is fluctuations of electronic states of the conduction band bottom and/or valence band top [43–45]. Apparently, the introducing of the co-dopant ions into GGAG lattice can induce some fluctuations in the electronic states of the crystal that we can see in the excitation spectra in Fig. 4. These data demonstrate different intensities of the excitation spectra in the spectral region corresponding to the band-to-band transitions (just higher the excitonic transitions) confirming our suggestion that co-doped crystals may have a distinguished thermalization length. Passing to the region of MEE the tendency remains the same, i.e. the samples having a higher excitation intensity at low energy range reveal stronger excitations in the MEE region and vice versa.

On the other hand, all single crystals studied in current research have some amount of intrinsic defects, some of them are responsible for the 5.3 eV excitation band. We suggest that these defects are efficient traps for hot charge carriers that leads to the diminishing of MEE processes, and, subsequently plays a negative role in scintillation performing. Furthermore, Figs. 4 and 6 show the anti-correlation of the MEE efficiencies and the intensities of the 5.3 eV excitation band, which is a defect related band as we supposed above. Indeed, the best excitation efficiency is observed in the Mg^{2+} co-doped crystal which has the smallest defect related excitation band at 5.3 eV. Moreover, it was established before that Mg^{2+} co-doping is effective for removing shallow electron traps due to oxygen vacancies or gallium deficiency [38]. It is supposed that the introducing of Mg^{2+} co-dopants into GGAG lattice suppresses intrinsic defects in question and can improve the efficiency of MEE processes and subsequently the scintillating performance of the GGAG:Ce single crystals.

Conclusions

The luminescence properties of cerium doped as well as co-doped GGAG single crystals have been investigated by means of the vacuum ultraviolet (VUV) excitation spectroscopy utilizing radiation from the undulator beamline (FinestBeaMS) of 3rd generation synchrotron facility MAX IV. These results were supported by XANES experiments identifying Ce^{3+} and Ce^{4+} centers in the co-doped GGAG crystals. The pioneering luminescence results have been obtained for the GGAG:Ce single crystals in VUV and soft X-ray excitation range. It was shown that GGAG:Ce single crystals having different co-dopant ions reveal distinguished efficiency of multiplication electronic excitations in VUV spectral range. Two models were proposed to explain the differences in the excitation efficiency for the crystals studied. The first one proposes that co-dopants can influence a thermalization length of geminate electrons and holes. Another one suggests that intrinsic defects in GGAG lattice are responsible for the capture of hot charge carriers leading to the degradation of the excitation efficiency in VUV spectral range. It is also suggested that the luminescence properties can be improved by the co-doping of Mg^{2+} ions suppressing intrinsic defects in GGAG:Ce single crystals, which are responsible for the excitation band at 5.3 eV as well as for the capture of hot charge carriers influencing the excitation region in VUV range and restricting scintillating performance of GGAG:Ce.

CRediT authorship contribution statement

Anna P. Kozlova: Formal analysis, Investigation, Writing - original draft. **Valentina M. Kasimova:** Formal analysis. **Oleg A. Buzanov:** Investigation, Resources. **Kirill Chernenko:** Methodology, Investigation, Writing - original draft. **Konstantin Klementiev:** Methodology, Investigation. **Vladimir Pankratov:** Conceptualization, Methodology, Investigation, Writing - review & editing.

Declaration of Competing Interest

The authors declare that they have no known competing financial interests or personal relationships that could have appeared to influence the work reported in this paper.

Acknowledgements

Authors gratefully acknowledge the financial support from the Latvian Science Council grant LZP-2018/2-0358. The research leading to this result has been supported by the project CALIPSO plus under the Grant Agreement 730872 from the EU Framework Programme for Research and Innovation HORIZON2020. The work of A.P.K. was supported by the Ministry of Science and Higher Education of the Russian Federation, state contracts No. 11.6181.2017/ITR.

References

[1] Lecoq P, Gektin A, Korzhik M. Inorganic Scintillators for Detector Systems: Physical Principles and Crystal Engineering. Springer; 2017.
[2] Morishita Y, Yamamoto S, Izaki K, et al. Performance comparison of scintillators for alpha particle detectors. Nucl Instrum Methods Phys Res A 2014;764:383–6.
[3] Alenkov V, Buzanov OA, Dosovitskiy G, et al. Irradiation studies of a multi-doped $Gd_3Al_2Ga_3O_{12}$ scintillator. Nucl Instrum Methods Phys Res A 2019;916:226–9.
[4] Lecoq P. Development of new scintillators for medical applications. Nucl Instrum Methods Phys Res A 2016;809:130–9.
[5] T. Kanai, M. Sato, I. Miura, H. Yamada, Oxide phosphor and radiation detector using IT and X-ray CT device, US Patent 7,076, 020 B2; 2006.
[6] Kamada K, Yanagida T, Endo T, et al. 2-inch size single crystal growth and scintillation properties of new scintillator Ce:$Gd_3Al_2Ga_3O_{12}$. IEEE Nucl Sci Symp Conf Rec 2011:1927–9.
[7] Kamada K, Endo T, Tsutumi K, et al. Composition engineering in cerium-doped (Lu, Gd)$_3$(Ga, A_l)$_5O_{12}$ single-crystal scintillators. Cryst Growth Des 2011;11:4484–90.
[8] Kamada K, Yanagida T, Endo T, et al. 2 inch diameter single crystal growth and scintillation properties of Ce:$Gd_3Al_2Ga_3O_{12}$. J Cryst Growth 2012;352:88–90.
[9] Kamada K, Pursa P, Nikl M, et al. Cz grown 2-in. size Ce:Gd_3(Al, Ga)$_5O_{12}$ single crystal; relationship between Al, Ga site occupancy and scintillation properties. Opt Mater 2014;36(12):1942–5.
[10] Kamada K, Nikl M, Kurosawa S. Alkali earth co-doping effects on luminescence and scintillation properties of Ce doped $Gd_3Al_2Ga_3O_{12}$ scintillator. Opt Mater 2015;41:63–6.
[11] Tyagi M, Meng F, Koschan M, et al. Effect of codoping on scintillation and optical properties of a Ce-doped $Gd_3Ga_3Al_2O_{12}$ scintillator. J Phys D Appl Phys 2013;46:475302.
[12] Nikl M, Yoshikawa A. Recent R&D trends in inorganic single-crystal scintillator materials for radiation detection. Adv Opt Mater 2015;3:463–81.
[13] Wu Y, Meng F, Li Q, Koschan M, Melcher CL. Role of Ce^{4+} in the scintillation mechanism of codoped $Gd_3Ga_3Al_2O_{12}$:Ce. Phys Rev Appl 2014;2:044009.
[14] Nikl M, Babin V, Pejchal J, et al. The stable Ce^{4+} center: a new tool to optimize Ce-doped oxide scintillators. IEEE Trans Nucl Sci 2016;63:433–8.
[15] Kozlova NS, Buzanov OA, Kasimova VM, et al. Optical characteristics of single crystal $Gd_3Al_2Ga_3O_{12}$:Ce. Mod Opt Elec Mater 2018;4:7–12.
[16] Shirmane L, Feldmann C, Pankratov V. Comparing the luminescence processes of YVO_4:Eu and core-shell YVO_4@YF_3 nanocrystals with bulk-YVO_4:Eu. Phys B: Condens Mater 2017;504:80–5.
[17] Kuzmanoski A, Pankratov V, Feldmann C. Energy transfer of the quantum-cutter couple Pr^{3+}–Mn^{2+} in CaF_2:Pr^{3+}, Mn^{2+} nanoparticles. J Lumin 2016;179:555–61.
[18] Tuomela A, Pankratov V, Sarakovskis A, et al. Oxygen influence on luminescence

properties of rare-earth doped $NaLaF_4$. J Lumin 2016;179:16–20.
[19] Shirmane L, Pankratov V. Emerging blue-UV luminescence in cerium doped YAG nanocrystals. Phys Status Solidi RRL 2016;10:475–9.
[20] Pankratov V, Osinniy V, Nylandsted Larsen A, Bech Nielsen B. Si, nanocrystals embedded in SiO_2: optical studies in the vacuum ultraviolet range. Phys Rev B 2011;83:045308.
[21] Grigorjeva L, Millers D, Grabis J, et al. Luminescence properties of ZnO nanocrystals and ceramics. IEEE Trans Nucl Sci 2008;55:1551–5.
[22] Pankratov V, Hoszowska J, Dousse J-Cl, et al. Vacuum ultraviolet excitation luminescence spectroscopy of few-layered MoS_2. J Phys Condens Matter 2016;28:015301.
[23] Rus patent 2646407, Single crystal with garnet structure for scintillation detectors and its manufacturing method. Official Publication of Federal Institute of Industrial Property. Bull. No. 7; 2018.
[24] Pankratov V, Pärna R, Kirm M, et al. Progress in development of a new luminescence setup at the FinEstBeAMS beamline of the MAX IV laboratory. Radiat Measur 2019;121:91–8.
[25] Pärna R, Sankari R, Kukk E, et al. FinEstBeaMS – a wide-range Finnish-Estonian beamline for materials science at the 1.5 GeV storage ring at the MAX IV Laboratory. Nucl Instrum Methods Phys Res A 2017;859:83–9.
[26] Klementiev K, Norén K, Carlson S, Sigfridsson Clauss KGV, Persson I, Laboratory MAXIV. The BALDER Beamline at the. J Phys Conf Ser 2016;712:012023.
[27] Shannon RD. Revised effective ionic radii and systematic studies of interatomic distances in halides and chalcogenides. Acta Crystallogr 1976;32:751–67.
[28] Babin V, Bohacek P, Grigorjeva L, et al. Effect of Mg^{2+} ions co-doping on luminescence and defects formation processes in $Gd_3(Ga, Al)_5O_{12}$:Ce single crystals. Opt Mater 2017;66:48–58.
[29] Ogiegło JM, Katelnikovas A, Zych A, Jüstel T, Meijerink A, Ronda CR. Luminescence and luminescence quenching in $Gd_3(Ga,Al)_5O_{12}$ scintillators doped with Ce^{3+}. J Phys Chem A 2013;117:2479–84.
[30] Sibczynski P, Iwanowska-Hanke J, Moszyński M, et al. Characterization of GAGG:Ce scintillators with various Al-to-Ga ratio. Nucl Instrum Methods Phys Res A 2015;772:112–7.
[31] Bartosiewicz K, Babin V, Kamada K, et al. Energy migration processes in undoped and Ce-doped multicomponent garnet single crystal scintillators. J Lumin 2015;166:117–22.
[32] Springis M, Pujats A, Valbis J. Polarization of luminescence of colour centres in YAG crystals. J Phys Condens Matter 1991;3:5457.
[33] Pankratov V, Chernov S, Grigorjeva L, et al. Luminescence properties and energy transfer processes in nanosized cerium doped YAG. IEEE Trans Nucl Sci 2008;55:1509–13.
[34] Babin V, Blazek K, Krasnikov A, et al. Luminescence of undoped LuAG and YAG crystals. Phys Status Solidi (c) 2005;2:97–100.
[35] Vrubel II, Polozkov RG, Shelykh IA, et al. Bandgap engineering in yttrium-aluminum garnet with Ga doping. Cryst Growth Des 2017;17:1863–9.
[36] Grazioli C, Hu Z, Knupfer M, et al. Characteristic temperature dependence of the 4f occupancy in the Kondo system $CeSi_2$. Phys Rev B 2001;63:115107.
[37] Mansuy C, Nedelec JM, Mahiou R. Molecular design of inorganic scintillators: from alkoxides to scintillating materials. J Mater Chem 2004;14:3274–80.
[38] Kitaura M, Kamada K, Kurosawa S, et al. Probing shallow electron traps in cerium-doped $Gd_3Al_2Ga_3O_{12}$ scintillators by UV-induced absorption spectroscopy. Appl Phys Exp 2016;9:072602.
[39] Blahuta S, Bessière A, Viana B, et al. Evidence and consequences of Ce^{4+} in LYSO:Ce, Ca and LYSO:Ce, Mg single crystals for medical imaging applications. IEEE Trans Nucl Sci 2013;60:3134–41.
[40] Ilmas ER, Liidya GG, Lushchik ChB. Photon multiplication in crystals. I. Luminescence excitation spectra of ionic crystals in the region 4 to 21 eV. Opt i Spektroskopiya 1965;18:453.
[41] Kirm M, Martinson I, Lushchik A, et al. Multiplication of anion and cation electronic excitations in wide-gap KCl and CsCl crystals. Solid State Commun 1994;90:741–4.
[42] Lushchik A, Kirm M, Lushchik Ch, et al. Multiplication of electronic excitations and prospects for increasing scintillation efficiency in wide-gap crystals. Nucl Instrum Methods Phys Res A 2005;537:45–9.
[43] Gektin AV, Belsky AN, Vasil'ev AN. Scintillation efficiency improvement by mixed crystal use. IEEE Trans Nucl Sci 2014;61:262–70.
[44] Belsky AN, Auffray E, Lecoq P, et al. Progress in the development of LuAlO/sub 3/-based scintillators. IEEE Trans Nucl Sci 2001;48:1095–100.
[45] Grigorjeva L, Millers D, Chernov S, Nikl M, Usuki Y, Pankratov V. The study of time-resolved absorption and luminescence in $PbWO_4$ crystals. Nucl Instrum Methods Phys Res B 2000;166–167:329–33.

Institute of Solid State Physics, University of Latvia as the Center of Excellence has received funding from the European Union's Horizon 2020 Framework Programme H2020-WIDESPREAD-01-2016-2017-TeamingPhase2 under grant agreement No. 739508, project CAMART²